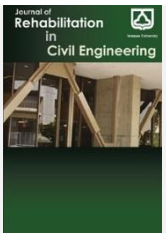

Journal of Rehabilitation in Civil Engineering

Journal homepage: https://civiljournal.semnan.ac.ir/

An Experimental Study on Bond Behavior of Rebar and High-Performance Fiber Reinforced Cementitious Composite (HPFRCC) at High Temperatures

Salim Karimpour[1]; Rahmat Madandoust [2,*]; Malek Mohammad Ranjbar [3*]; Habib Akbarzadeh Bengar [4]

1. Ph.D. Student, Department of Civil Engineering, University of Guilan, Rasht, Iran
2. Professor, Department of Civil Engineering, University of Guilan, Rasht, Iran
3. Associate Professor, Department of Civil Engineering, University of Guilan, Rasht, Iran
4. Associate Professor, Department of Civil Engineering, University of Mazandaran, Babolsar, Iran

* Corresponding author: *ranjbar@guilan.ac.ir*

ARTICLE INFO

Article history:
Receive Date: 09 February 2023
Revise Date: 11 April 2023
Accept Date: 05 July 2023

Keywords:
Bond behavior;
HPFRCC;
PVA fibre;
RILEM test;
Pullout test.

ABSTRACT

In this work, it was attempted to explore the bond behavior of rebars in high-performance fiber-reinforced cementitious composite (HPFRCC) consisting of hybrid fibers with 1 and 2% by weight of binder for steel and 0.1, 0.2, 0.3, and 0.4% by weight of binder for polypropylene (PP) and polyvinyl alcohol (PVA) fibers along with the compressive and tensile strengths after exposure to high temperature. From 19 mix designs, four superior ones which experienced lower reduction in compressive strength at 400 and 600 ^{o}C was selected in order to investigate the bond behavior of rebar in HPFRCC specimens using direct pullout and RILEM beam tests. The experimental results revealed that the HPFRCC specimens with 1% steel fiber combined with 0.2% PP fiber and 0.3% PVA fiber, separately, had the minimum compressive strength loss at 400 and 600 °C. For the HPFRCC with 2% steel fiber, the higher compressive strength at the given temperatures was observed for those with 0.3% PP and 0.2% PVA fiber, separately. The specimens with higher compressive strength at the given temperatures were those that had 2% steel fibers, 0.3% PP, and 0.2% PVA fibers. The specimen with 1% steel fibers and 0.3% polypropylene fibers had a greater tensile strength with a value of 14.2 MPa compared to other specimens. Furthermore, the bond capacity of rebar in HPFRCC continues to decline with temperature rise up to 600 °C to the point where this reduction for the chosen specimens is approximately 62% of the bond strength of the specimens at the room temperature (i.e., 23 °C). The maximum pull-out force has a significant relationship with the type and proportion of fibers, as demonstrated by the RILEM beam's results. Compared to specimens containing PP fibers, those with PVA fibers at high temperatures were able to tolerate higher bond strength.

E-ISSN: 2345-4423

How to cite this article:
Karimpour, S. , Madandous, R. , Ranjbar, M. M. and Akbarzadeh Bengar, H. (2024). An Experimental Study on Bond Behavior of Rebar and High-Performance Fiber Reinforced Cementitious Composite (HPFRCC) at High Temperatures. Journal of Rehabilitation in Civil Engineering, 12(1), 77-91.
https://doi.org/10.22075/jrce.2023.29856.1810

1. Introduction

The concrete-steel rebar bond capacity plays an important role in the ultimate loading capacity of a reinforced concrete member. This parameter also affects a number of serviceability design criteria including crack width, crack spacing, and deflection of the member[1–4]. ACI-408R-03[5] states that the force transfer between a deformed rebar and surrounding concrete occurs through (a) chemical bond between the rebar and concrete that depends on the surface texture of the rebar and the type of concrete; (b) friction between the rebar and the concrete that is controlled by interfacial roughness, normal forces on the rebar surface, and rebar-concrete relative slip ; and (c) mechanical interlocking between the rebar ribs and concrete.

The direct pullout and the beam-bending tests as the most commonly used techniques for investigating the concrete-steel rebar bond were used according to the recommendations of RILEM[1]-7-II-128 [1] and RILEM-7-II-28D [6] as proposed by many researchers like Chan et al .[7], Belarbi et al. [8], Desnerck et al. [9], Kotynia [10], Almeida Filho et al. [11], Mazaheripour et al. [12], and Deng et al. [13].

In the direct pullout test, a cylindrical concrete specimen with a known rebar bond length is loaded with the rebar location being either concentric or eccentric. This test is selected due to multiple reasons that include fabrication and testing simplicity and the ability to isolate various variables impacting the overall bond performance[14].

Many studies have addressed he rebar-concrete bond behavior using the pullout or pushout tests [14–17]. Generally, the bond capacity is mainly a result of chemical adhesion, mechanical interlocking between the rebar ribs and concrete, and rebar-concrete friction after debonding[18–21]. Before debonding, mechanical interlocking is usually the governing mechanism for deformed rebars and mainly is a function of the mechanical capacity of concrete [12,13]. Upon pulling the rebar, the interlocking effect leads to shear stresses in concrete along the distance between the lateral rebar ribs and tensile stresses in concrete that leads to the lateral confinement of the rebar [14,19]. The rebar pullout from concrete leads to either concrete splitting failure or concrete shear failure (rebar pullout) [12], depending on different factors including the rebar dimensions and shape [15], compressive capacity of concrete [22], rebar embedment length [23], and concrete cover thickness [16,24]. Thus, it is expected that a higher mechanical capacity of concrete improves the bond capacity. Nevertheless, at elevated temperatures, the mechanical strength of concrete experiences significant degradation [25].

Different high-performance fiber-reinforced cementitious composites (HPFRCC) have been produced in recent years with the aim of reaching improved mechanical capacities. For example, ultra-high-performance concrete (UHPC) containing micro steel fibers was developed to reach high compressive and strength strengths [26–28]. Typically, a very small water/cementitious materials ratio (w/cm < 0.25) is used to produce UHPC ; this gives rise to a refined microstructure with low permeability and porosity , which in turn results in improved mechanical capacity and durability. Nevertheless, as reported by a number of researchers, the water vapor

[1] *International Union of Laboratories and Experts in Construction Materials, Systems, and Structures*

pressure accumulation occurs at high temperatures due to low permeability and leads to potential explosive spalling [24,29]. With temperature rise, more water is evaporated, which largely increases the pore pressure and internal stresses. In addition, cement hydrates decompose, leading to increased water quantity and reduced mechanical capacity of concrete [30,31]. However, HPFRCC has the successful performance in the room temperature, it is necessary to study the mechanical properties and bond strength between HPFRCC and rebars under the elevated temperatures, according which is rarely considered in the literatures.

Li et al. [14] studied bond capacity of steel rebars in high-performance fiber-reinforced cementitious composite before and after heating. They found that as the rebar diameter increased from 12 to 20 mm, the bond capacity declined by up to 55% at 800 °C. It was also reported that as the rebar bond length increased from 40 to 100 mm, bond capacity declined by up to 55% at 800 °C. Yoo et al. [18] investigated the bond performance of steel rebar embedded in ultra-high-strength concrete. Experimental data indicated that increasing the compressive capacity of concrete considerably increased the average bond strength and increasing the bar size slightly decreased this parameter . Yoo et al. [32] carried out an experimental study on pullout and tensile behavior of ultra-high-performance concrete reinforced with various steel fibers. Their achievements showed that maximum pullout forces occurred in specimens containing twisted and half-hooked steel fibers with aligned and highly inclined orientation, respectively. Additionally, straight steel fibers showed the best tensile behavior in UHPFRC is , and twisted, half-hooked, and hooked steel fibres demonstrated the next best behaviors. Krahl et al. [33] studied the impact of curing age on the pullout performance of inclined and aligned steel fibers in UHPFRC. Based on the results, inclined fibers showed the largest bond capacities at 28 d due to the snubbing impact, and the interfacial bond of straight fibers increased exponentially with age.

According to the aforementioned discussion, the main objective of the present study is to experimentally investigate the bond behavior between rebar and HPFRCC under elevated temperatures, i.e., 400 and 600 ^{o}C using direct pullout and RILEM tests which is firstly carried out in current research. Additionally, the simultaneous effect of steel fiber with each polyvinyl alcohol fibre (PVA) and polypropylene (PP) fibers by different percentages is investigated in term of compressive and splitting tensile strengths before and after exposing elevated temperature.fibersIn this study, the design parameters including type and the percentage of fibres in HPFRCC using direct pullout and beam-bending tests based on RILEM is considered.

2. Materials and methods

2.1. Material properties

The sand employed in this study, which has a maximum size of 0.6 mm, a density of 2.51 gr/cm^3, and a water absorption rate of 3.9%, was manufactured from Hamadan mines. The sieve analysis of sand, which showed that it was within the permitted range established by the ASTM C778 standard, are displayed in Table 1. Type II Hemagethan cement with the chemical and physical properties listed in

Table 2 was utilized to create HPFRCC specimens.

Table 1. Results of the sand grading.

Weight of retained (Passing percentage)	Sieve size	Sieve No
0 (100)	1.18	#**16**
0 (100)	0.85	#**20**
22 (97)	0.6	#**30**
256 (68)	0.42	#**40**
419 (24)	0.3	#**50**
130 (3)	0.15	#**100**

Additionally, Table 2 displays the physical and chemical properties of the Semnan silica fume (used in this experiment). The generated silica fume complies with ASTM C150 standards, and for this study, sieve No. 30 was used to manage appearance traits and guarantee lump-free materials.

Table 2. Chemical compositions of binder materials.

Oxide	Cement	Silica fume
SiO_2	19.9	85
Al_2O_3	5.91	1
Fe_2O_3	2.10	2
CaO	62.92	1.5
MgO	1.25	2
Na_2O	0.38	-
K_2O	0.9	-
SO_3	3.26	-
Cl-	0.011	-
C	-	3
Loss On Ignition	3.94	3.5

The retarder super-plasticizer modified with the commercial code of FARCO PLAST P10-3R from the Construction Chemical Company is utilized in the research's mix designs. It complies with ASTM C494-Type G standards and has modified polycarboxylate as its chemical foundation. The stainless alloy steel employed in this study has a commercial designation of 304 and is developed by the Azma Sanat Sazan Narun Company specifically for use in fine-grained cement composites. PVA fibers were produced by Kuraray in Japan for this investigation. Additionally, Ramka Construction Chemical Industries prepares the PP fibers used in concrete, which are specifically employed in all varieties of fiber concrete. Figure 1 and Table 3 shows the physical and mechanical properties of the various fiber types used in this study.

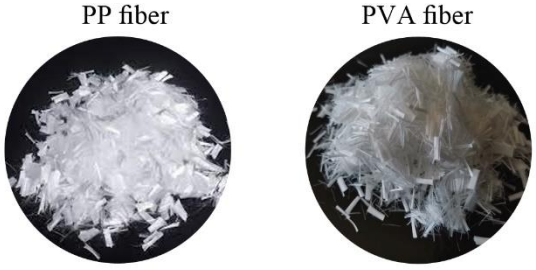

Fig. 1. Used PP and PVA fibres in the current study.

Table 3. Specifications of the fibers(results are from the company).

Fibre	Steel	PP	PVA
Diameter (mm)	0.2	0.035	0.013
Length (mm)	13	6	6
Tensile strength (MPa)	620	400	1600
Density (gr/cm^3)	7.85	0.91	1.3

2.2. Mix design and specimen preparation

The laboratory specimens were created in the shapes of 10 × 20 mm cylinders for pullout tests and cubic specimens of 10 × 10× 10 cm for compressive strength testing. Two HPFRCC beams with dimension of 10×18×38 cm were made to serve as specimens for the RILEM beam flexural test, and they were inserted into the lower portion of the concrete specimen by a ribbed rebar for flexural performance. In addition, the cylindrical specimens with dimensions of 10×20 were made for the indirect tensile test (bisection). Nineteen mix designs that were created in three sections were taken into consideration for the initial stage of this investigation. In the first series, the effect of each steel fiber percentage (1 and 2%) was measured

separately, according which the optimum percentage of steel fiber was proven by researchers from 0.5 to 2.5% [34,35]. In the second series, fixed percentages of these fibers were considered to study their simultaneous effect with polymer fibers during thermal operations, and the percentages of 0.1, 0.2, 0.3, and 0.4 of PVA fiber were regarded as polymer supplements for steel fibres. Polypropylene fiber were considered supplements in the third series at the rates of 0.1, 0.2, 0.3, and 0.4%. This percentage of fiber addition is controversial among researchers [13,36–38].The amounts of cement (907 kg), silica fume (181 kg), water-cement materials ratio (0.25), and fine grains (927 kg) were considered constants in all mix designs. Table 4 provides the quantities and ratios of each component of the examined mixtures. It should be noted that three specimens were prepared for each of the mix designs to test the compressive and tensile strengths, and the mean values of the data were presented in this study.

The introduced ingredients were mixed using a vane mixer to create HPFRCC mortars. Dry ingredients are initially combined at a slow speed (30 rpm) until the silica fume in the cement and sand combination entirely vanishes and a significant volume reduction is observed in the dry mixture. The mixture is then mixed for 1 minute at a low speed (30 rpm) with a minimum amount of super-plasticizer (0.003), and the efficacy of the mixture is managed using standard techniques (such as a flow table). To achieve the required distribution (based on the mixture's appearance), fibers are added to the mixture in a series of phases (up to five in total), and the mixing is then maintained at a high speed for 4 to 6 minutes. Finally, the mixture is then given a further 5% addition of water (if necessary), along with the second segment of the super-plasticizer, and is stirred at a high speed for an additional two minutes (70 rpm). Zoning the new mixture into equal sections and visual inspection to ensure there are no fiber masses in the mixture are the criteria for proper fiber distribution in this mix design.

Table 4. Mix design of specimens.

Mix Code	W/B	SF	SP	Steel	PP	PVA
C	0.25	181	4.352	0	0	0
HS10	0.25	181	5.44	78.5	0	0
HS20	0.25	181	7.616	157	0	0
HS10V01	0.25	181	6.528	78.5	0	2.6
HS10V02	0.25	181	6.528	78.5	0	5.2
HS10V03	0.25	181	7.616	78.5	0	7.8
HS10V04	0.25	181	7.616	78.5	0	1.3
HS10P01	0.25	181	5.44	78.5	0.91	0
HS10P02	0.25	181	6.528	78.5	1.82	0
HS10P03	0.25	181	7.616	78.5	2.73	0
HS10P04	0.25	181	7.616	78.5	3.64	0
HS20V01	0.25	181	7.616	157	0	1.3
HS20V02	0.25	181	8.704	157	0	2.6
HS20V03	0.25	181	9.792	157	0	3.9
HS20V04	0.25	181	9.792	157	0	5.2
HS20P01	0.25	181	8.704	157	0.91	0
HS20P02	0.25	181	9.792	157	1.82	0
HS20P03	0.25	181	9.792	157	2.73	0
HS20P04	0.25	181	10.88	157	3.64	0

The specimens were molded and compacted on the vibrating table following the mixing of the concrete mixture. Then, they were placed in the mold and kept with their surfaces continuously wet for approximately 24 hours. Subsequently, they were cured inside the water basin after being removed from the mold until

they reached the required age for the tests. Finally, the prepared specimens for the RILEM beam test are shown in Figure 2.

Fig 2. Prepared HPFRCC beam for beam-bending test.

2.3. Compressive strength test

The compressive strength was evaluated using cube specimens. In this test, the compressive loading rate is 2 kN/s or 0.25 MPa/s. In this study, HPFRCC specimens were used to examine the curing process under standard settings and after thermal operations at high temperatures.

2.4. Splitting tensile strength test

The tensile strength of concrete by bisection technique or Brazilian test is the term given to this test in the ASTM C496 standard. In this test, the specimen is positioned between the breaker jack's plates with its axis horizontal. The load is then raised until the specimen failure—a splitting in half—occurs in the plane encompassing its vertical diameter. According to ASTM C496-90 guidelines, thin plywood strips with a thickness of 3 mm, a width of 25 mm, and a length equivalent to that of the mold should be used to prevent the development of extremely high local compressive stresses in the loading lines.

2.5. Direct pullout test

The pullout test was carried out using a universal testing machine (UTM) having a capacity of 250 kN. The bottom steel plate of the steel frame supports the specimens vertically throughout this test, and the lower jaw of the testing apparatus receives the longer end of the rebar that has been driven through the concrete. This is happening as the device's top arm pulls the steel frame and the specimen cube within (Figure 3). The relative displacement of the rebar around the concrete was measured using an LVDT positioned in the shortest portion of the end of the rebar (sliding). For steel rebar with a diameter of 16 mm, the pullout rate using the device was deemed to be equivalent to 128 N/s, as stated in the RILEM RC6 standard [6].

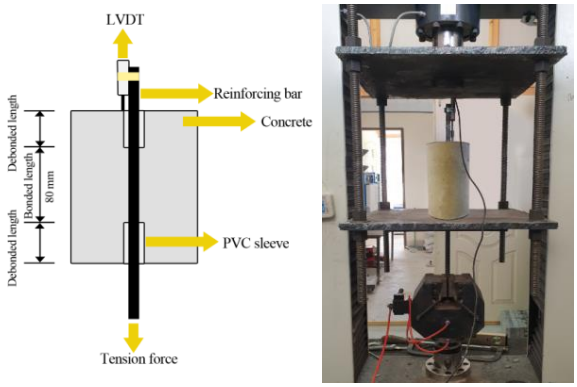

Fig 3. Schematic illustration of direct pullout test.

2.6. RILEM beam test

According to [10], middle separation cracks should be studied using the RILEM beam method, whereas end separation and important diagonal fractures should be studied using the Pullout method. The specifications of the beam used in this study to analyze the RILEM standard-based bonding are shown in Figure 4. Rebar slip in UPFRCC has been measured using three LVDT transducers at both the

loading site and the two free ends of the rebar. The installed displacement between the free end of the rebar and the surface of the HPFRCC rear section is measured by LVDTs 1 and 2, which are installed at the two ends of the rebar, respectively. Additionally, LVDT 3 is positioned on the unobstructed portion of the rebar in block A to measure the installation displacement between this section and the HPFRCC surface. To measure the amount of load delivered to each segment of the beam specimen connection, three load cells with a combined capacity of 200 kN have been placed.

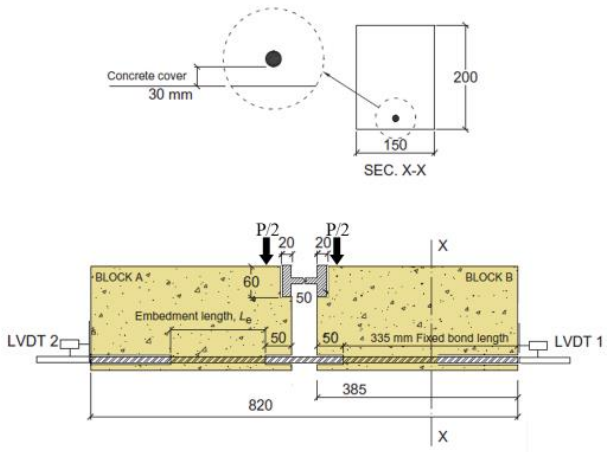

Fig 4. Schematic illustration of RILEM beam test.

2.7. Heat implementation method

After being dried for 48 hours at 110 °C in a hothouse, the HPFRCC specimens were put in a laboratory gas furnace that was set up for thermal operations with a temperature increase rate of 5 degrees per minute. The maximum temperatures were considered 400 and 600 °C, and when they reached such temperatures, they were maintained there for two hours with a tolerance of 3 °C. Then, it was gradually cooled, and tests on the heated specimens were run after 24 hours. The examples of HPFRCC beams for using high temperatures in the furnace are shown in Figure 5.

Fig 5. High-temperature furnace.

3. Results and discussion

3.1. Compressive strength test

In this study, all mixes underwent a compressive strength test after 28 days. Figure 6 displays the results of this test for the HPFRCC specimens at 23°C, 400°C, and 600°C. These values represent the mean results of compressive strength for three specimens. Based on these findings, the HS20 test, which contains 2% steel fibres, has a 28-day compressive strength that is approximately 5% higher than the HS10 test.

The HS20P01 test, which had a compressive strength of 119.8 MPa for specimens with PP fibres, and the HS20V01 test, which had a compressive strength of 121.3 MPa for specimens with PVA fibres, had the highest performance. Due to its 0.1 and 0.2% relative compressive strengths, this specimen has the maximum performance. According to the findings, if PP and PVA fibre volume is employed more than a particular level, the fibres not only have no impact on enhancing compressive strength but also result in a drop in strength[39,40]. These specimens were heated to temperatures between 400 and 600 °C to investigate one of the most significant objectives of this research, which is to investigate the strength performance of the

specimens under high heat. At this point, the best mix designs are considered for the pullout test. The specimens were therefore examined for compressive strength after being subjected to heat of 400 and 600 °C for two hours and cooling for 24 hours. According to the findings shown in Figure 7, the steel fibre group saw a 0.3% drop in compressive strength at 400°C, whereas the specimens comprising 0.2% PP fibre and 0.3% PVA experienced a 0.3% decrease.

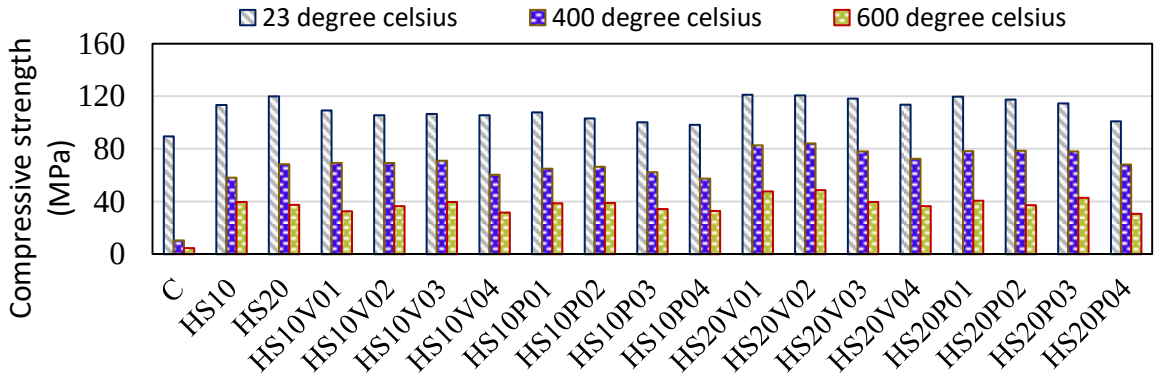

Fig. 6. Compressive strength results for HPFRCC specimens under room and high temperature.

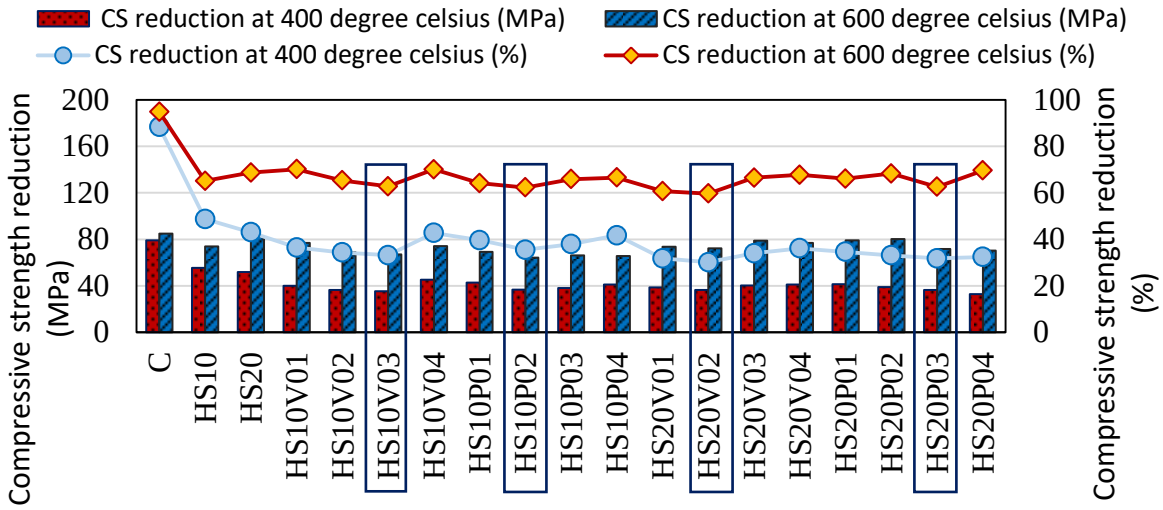

Fig. 7. Residual compressive strength values along with its percentages for HPFRCC specimens under room and high temperature.

For instance, the compressive strength at 400 °C for the HS10V03 specimen, which had 0.3%, was 35.5 MPa, but this decline rate for the HS10 specimen, which lacked polymer fibres, is equivalent to 53.5 MPa. This demonstrates that the inclusion of PP maintains the strength properties of concrete, particularly its compressive strength at high temperatures, and concrete containing fibre like PP or PVA will have less loss in structural performance. However, it is crucial to understand the optimal rate to use when adding these fibres fibre to concrete. The selection criteria for the HS20P03 and HS20P04 specimens at 400 °C might appear a little stringent, however, at 600 °C, the percentage of compressive strength loss for the specimen with 0.3% PP fibre was lower than the specimen with 0.4% PP fibres. As a consequence, four mix designs for the rebar pullout test from concrete are chosen in the next section based on the findings from

exposing the specimens to 400 and 600 °C temperature and considering each of the best mix designs in this study. These four mix designs are HS10V03, HS10P02, HS20V02, and HS20P03, as displayed in Figure 6.

3.2. Tensile strength test

Figure 8 displays the results of the tensile strength test (bisection) performed on 28-day HPFRCC specimens at temperatures of 23, 400, and 600 °C. The specimen comprising 1% steel fibre and 0.3% PP fibre had a greater tensile strength than the other specimens with a value of 14.2 MPa at the 23 °C room temperature. In a quantitative comparison between PVA fibre at a rate of 0.3% and PP fibre at a rate of 0.2%, the results demonstrate that PVA fibre aid to raise the tensile strength by 2.5% when the volume percentage of steel fibre is held constant (2%). The tensile strength of the HPFRCC specimens decreased significantly as the temperature was raised to 400 °C. As a result, the tensile strength of specimens containing PP, such as HS10P02 and HS20P03, has fallen by 48 and 42%, respectively, whereas specimens containing PVA, such as HS10V03 and HS20V02, have reported a value of approximately 32%. The HPFRCC specimens have been placed at a temperature of 600 °C to attain their lowest point. For instance, when the temperature was raised for the HS10P02 specimen, the tensile strength reduced from 12.7 MPa at the room temperature to 4.58 MPa at 600 °C, which is a 64% reduction in the specimen's tensile strength.

Accordingly, comparing PVA and PP fibres, HPFRCC specimens with PVA fibre have considerably lower compressive strength at high temperatures.

3.3. Pullout test

To determine the mean bond stress over the length of the rebar installed in concrete using the tensile force in the pullout test, the RILEM RC6 standard [21] has recommended the following equation:

$$\tau_b = \frac{F}{5\pi d_s^2} \quad (1)$$

The ACI 408 standard [23] divides the parameters that affect bond strength into three categories: structural parameters (concrete cover, development length), concrete-related parameters (compressive and tensile strengths, workability, type of aggregate), and rebar-related parameters (yield stress, ultimate stress, modulus of elasticity). One of the primary objectives of this study is to assess how temperature and the rate of PP and PVA fibres affect the bond strength between rebar and concrete in the pullout test. Figure 9 depicts the way of pulling out the rebars from the fiber specimen. Since the compressive strength and bond strength are directly correlated, the specimens containing 2% steel fibre had a 9% greater bond strength. The findings indicate that the use of PVA or PP fibre has little impact on the bond strength of HPFRCC specimens and rebar, practically at a room temperature, and that the degree of bonding increase in the PVA specimens cannot be used as a criterion for decision-making in this study.

The findings of applying heat to fibre concrete specimens reveal that doing so decreased the binding strength of the HS10V03 specimen by 7.4 and 5.13 percent, respectively, and that the rebar-concrete bonding was reduced by 39 and 64 percent. This decreased rate is 53 and 68%, respectively, for the HS10P02 specimen. The results in Figure 8 demonstrated that the specimen containing PP fibre had a sudden

drop in high temperatures with the same quantity of steel fibres. The bonding performance of rebar and HPFRCC specimens in specimens containing 2% steel fibre indicated that with rising temperatures up to 400 °C, the bonding loss with PP fibre was around 38%, whereas this decrease was only about 26% for specimens with PVA fibres.

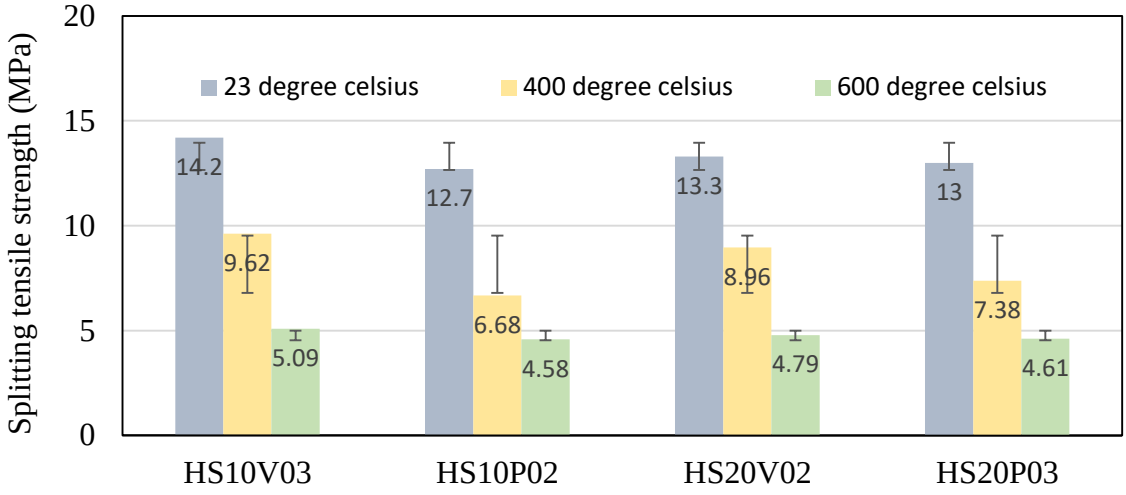

Fig. 8. Splitting tensile strength for HPFRCC specimens under room and high temperature.

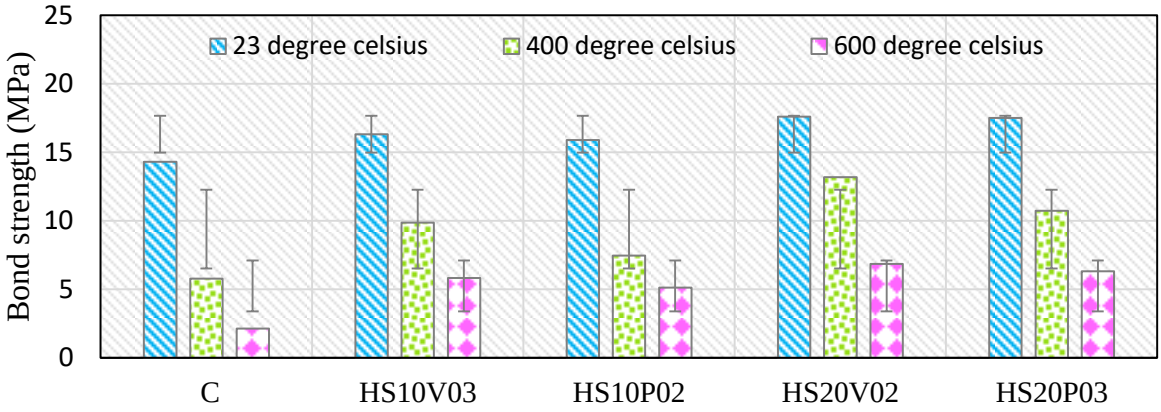

Fig. 9. Pullout test results for bond strength between rebar and HPFRCC under room and high temperature.

This indicates that PVA fibre outperform the PVA fibre when it comes to concrete-rebar bonding when subjected to the temperature. The bond strength of HPFRCC specimens continues to deteriorate at temperatures up to 600°C, and for the chosen specimens, this decline equals around 62% of the bond strength of the materials at an room temperature (i.e. 23 °C). According to literature [41], the failure mode of specimens containing PVA switches from separation to pullout when 2% of steel fibre are added, and this bond strength rises to more than 10%. In addition, the bond strength of HPFRCC specimens was raised by almost 17% by increasing the steel fibre from 1% to 2% at 600 °C. Indeed, the interaction and involvement of fibres, particularly steel fibres, begins and stops microcracks until the crack width develops when microcracks develop in specimens as a result of tensile stress.

3.4. RILEM beam test

Figure 10 displays the findings of the bonding rate of ribbed rebar in HPFRCC specimens using the RILEM beam test at 23, 400, and

600 °C based on the relationship between the bonding force and displacement. In cases when the damage to the beam during the rebar pullout process is not severe enough to result in an irreversible slip, the tensile force versus displacement or slip responses are often represented by a short linear branch. Then, due to the rise in damage, the trend in transferring this load till the peak loading period follows this nonlinear pattern. A downward branch of tensile force with increasing displacement characterizes the post-peak stage. The maximum pullout force is significantly correlated with the kind and proportion of fibre utilized, as shown in Figure 10. This number for the HPFRCC specimens that included PVA enhanced the rebar in the specimens' bond strength. For instance, the specimen's maximum pullout load in this test is 17.87 MPa, and the matching rebar's displacement under loading is similarly 0.128%.

According to the findings, the mean bond strength of the rebar with the HPFRCC specimens has fallen by 45% when the temperature is raised to 400 °C. Furthermore, specimens with PVA fibre could support greater bonding forces than PP specimens at this temperature. The bond strength obtained was 10.86 for the HS20V02 specimen, decreasing 40% from the room temperature, whereas this value has been measured at 46% for the HS20P03 specimen. The general behaviour of the beam has not changed considerably from 400°C to 600°C in the load-displacement diagram, but the form of the curves has modified, as opposed to the figure's slope. Moreover, Figure 10 displays the ribbed rebar's maximum bond strength using HPFRCC specimens at 23, 400, and 600 °C.

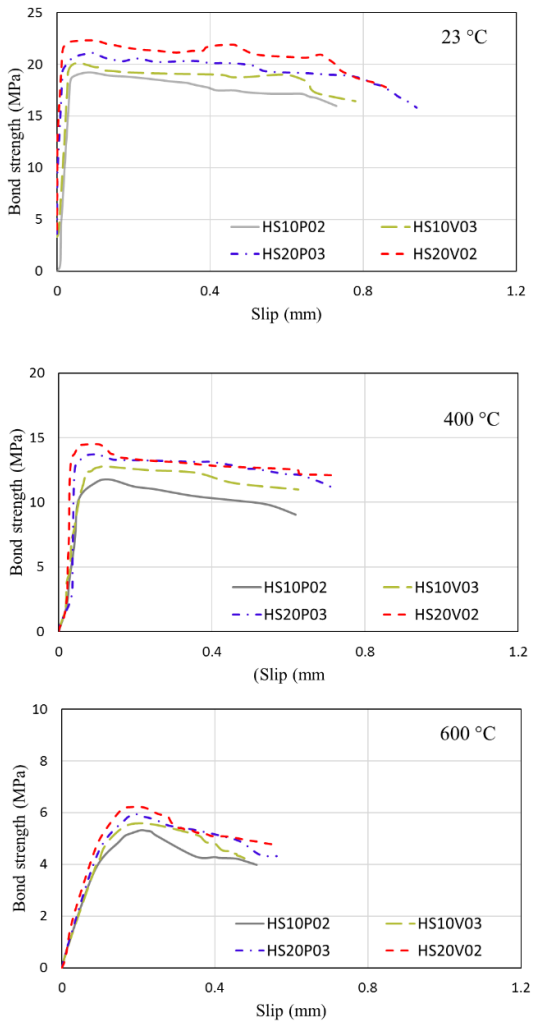

Fig 10. RILEM beam test of HPFRCC results for 23, 400, and 600 °C.

3.5. Comparison between pullout and RILEM beam test

Due to the presence of transverse reinforcement, the concrete is confined to prevent a splitting failure and thus develops higher bond stress causing bar pullout failure. Therefore, bond capacity values in the RILEM beam test with transverse rebars are greater than those obtained in the pullout test. It is seen in Figure 11 comparing the bond capacity values of HPFRCC specimens in different temperatures. At 23°C, the RILEM bond strength was on average 1.23 times greater than the bond strength values obtained from pullout test.

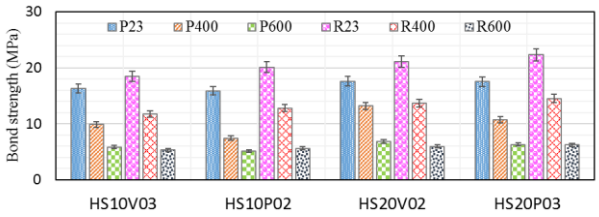

Fig 11. Pullout and RILEM beam test results in 23, 400, and 600 °C (P and R stand for pullout and RILEM, respectively).

4. Conclusion

In this study, the mechanical properties of these specimens, including the compressive strength and tensile strength of specimens exposed to elevated temperatures, were analysed together with the bond strength of rebar and HPFRCC. Considering the experimental results, it is concluded that:

1. Of the 19 mix designs suggested by this study, The specimens with 0.2% PP fibre and 0.3% PVA had the minimum compressive strength loss at 400°C compared to the 1% steel fibre group. For instance, the compressive strength of the specimen HS10V03, which contains 0.3% PVA fibres, was 35.5 MPa at 400 °Cfibers.

2. fibersfibersIn a quantitative comparison between PVA fibre at a rate of 0.3% and PP fibre at a rate of 0.2%, the results demonstrate that PVA fibre aid to raise the tensile strength by 2.5% while keeping the percentage of steel fibre unchanged. The tensile strength of the HPFRCC specimens decreased significantly as the temperature was raised to 400 °C. As a result, HS10P02 and HS20P03 specimens that include PP have a lower tensile strength by 48% and 42%, respectively. This value is stated to be around 32% for specimens containing PVA, such as HS10V03 and HS20V02. Accordingly, HPFRCC specimens with PVA fibre had considerably lower compressive strength at high temperatures than HPFRCC specimens with PP fibres.

3. The direct pullout test findings indicate that, with the same quantity of steel fibres, the specimen containing PP fibre had a sharp drop at high temperatures. With temperature increases up to 400 °C, the bonding performance of rebar in HPFRCC specimens containing 2% steel fibre was such that the loss of bonding with PP fibre was only around 38%. However, this rate for the specimens containing PVA fibres is around 26% reduction, indicating that PVA fibres perform better when subjected to temperature than PVA fibres. The bond strength of rebar and HPFRCC specimens continues to deteriorate when the temperature is raised to 600 °C, and for the chosen specimens, this loss is approximately 62%.fibers

4. The maximum pullout force has a significant relationship with the type and percentage of fibres, as indicated in the RILEM beam test results, and this value for the HPFRCC specimens that contained PVA indicates a rise in the rebar bond strength in the specimens. For instance, the specimen's highest bond strength in this test is 17.87 MPa, and the equivalent rebar's displacement under load is 0.128 mm. According to the findings, the bond strength between the rebar and the HPFRCC specimens was reduced by an average of 45% when the temperature was raised to 400 °C. fibersIn the load-displacement diagram, the general behaviour of the beam has not changed considerably from 400°C to 600°C, but the form of the curves has modified, as opposed to the figure's slope.

References

[1] Bažant ZP, Li Z, Thoma M. Identification of Stress-Slip Law for Bar or Fiber Pullout by Size Effect Tests. J Eng Mech 1995;121:620–5. https://doi.org/10.1061/(asce)0733-9399(1995)121:5(620).

[2] Bingöl AF, Gül R. Residual bond strength between steel bars and concrete after elevated temperatures. Fire Saf J 2009;44:854–9. https://doi.org/10.1016/j.firesaf.2009.04.001.

[3] Bandelt MJ, Billington SL. Bond behavior of steel reinforcement in high-performance fiber-reinforced cementitious composite flexural members. Mater Struct Constr 2016;49:71–86. https://doi.org/10.1617/s11527-014-0475-4.

[4] Jahangir H, Nikkhah Z, Eidgahee DR, Esfahani MR. Performance Based Review and Fine-Tuning of TRM-Concrete Bond Strength Existing Models. J Soft Comput Civ Eng 2023;7:43–55. https://doi.org/10.22115/scce.2022.349483.1476.

[5] Institute) ACI (American C. ACI 408R-03: Bond and development of straight reinforcing bars in tension, 2003.

[6] Rilem TC. RC 6 Bond test for reinforcement steel. 2. Pull-out test, 1983. RILEM Recomm Test Use Constr Mater 1994:218–20.

[7] Chan Y-W, Chen Y-S, Liu Y-S. Development of bond strength of reinforcement steel in self-consolidating concrete. Struct J 2003;100:490–8.

[8] Belarbi A, Richardson DN, Swenty MK, Taber LH. Effect of Contamination on Reinforcing Bar-Concrete Bond. J Perform Constr Facil 2010;24:206–14. https://doi.org/10.1061/(asce)cf.1943-5509.0000091.

[9] Desnerck P, Lees JM, Morley CT. Bond behaviour of reinforcing bars in cracked concrete. Constr Build Mater 2015;94:126–36. https://doi.org/10.1016/j.conbuildmat.2015.06.043.

[10] Kotynia R. Bond between FRP and concrete in reinforced concrete beams strengthened with near surface mounted and externally bonded reinforcement. Constr Build Mater 2012;32:41–54. https://doi.org/10.1016/j.conbuildmat.2010.11.104.

[11] Almeida Filho FM, El Debs MK, El Debs ALHC. Numerical approach of the bond stress behavior of steel bars embedded in self-compacting concrete and in ordinary concrete using beam models. Rev IBRACON Estruturas e Mater 2013;6:499–512. https://doi.org/10.1590/s1983-41952013000300009.

[12] Mazaheripour H, Barros JAO, Sena-Cruz JM, Pepe M, Martinelli E. Experimental study on bond performance of GFRP bars in self-compacting steel fiber reinforced concrete. Compos Struct 2013;95:202–12. https://doi.org/10.1016/j.compstruct.2012.07.009.

[13] Deng F, Ding X, Chi Y, Xu L, Wang L. The pull-out behavior of straight and hooked-end steel fiber from hybrid fiber reinforced cementitious composite: Experimental study and analytical modelling. Compos Struct 2018;206:693–712. https://doi.org/10.1016/j.compstruct.2018.08.066.

[14] Li X, Bao Y, Xue N, Chen G. Bond strength of steel bars embedded in high-performance fiber-reinforced cementitious composite before and after exposure to elevated temperatures. Fire Saf J 2017;92:98–106. https://doi.org/10.1016/j.firesaf.2017.06.006.

[15] Xiao J, Hou Y, Huang Z. Beam test on bond behavior between high-grade rebar and high-strength concrete after elevated temperatures. Fire Saf J 2014;69:23–35. https://doi.org/10.1016/j.firesaf.2014.07.001.

[16] Kim SW, Yun H Do, Park WS, Jang Y Il. Bond strength prediction for deformed steel rebar embedded in recycled coarse aggregate concrete. Mater Des 2015;83:257–69. https://doi.org/10.1016/j.matdes.2015.06.008.

[17] Jahangir H, Rezazadeh Eidgahee D, Esfahani MR. Bond strength characterization and estimation of steel fibre reinforced polymer-concrete composites. Steel Compos Struct 2022;44.

[18] Yoo DY, Kwon KY, Park JJ, Yoon YS. Local bond-slip response of GFRP rebar in ultra-high-performance fiber-reinforced concrete. Compos Struct 2015;120:53–64.

https://doi.org/10.1016/j.compstruct.2014.09.055.

[19] Pothisiri T, Panedpojaman P. Modeling of bonding between steel rebar and concrete at elevated temperatures. Constr Build Mater 2012;27:130–40. https://doi.org/10.1016/j.conbuildmat.2011.08.014.

[20] Wei J, Liu H, Leung CKY. Numerical modelling of bond behavior between rebar and high-strength fiber-reinforced cementitious composites (HSFRCC) for inter-module joint in modular construction. Eng Struct 2023;278:115483. https://doi.org/10.1016/j.engstruct.2022.115483.

[21] Elhadary R, Bassuoni MT. Interfacial Bonding between Basalt Fiber/Polymer Pellets and Various Nano-Modified Cementitious Matrices. J Mater Civ Eng 2023;35:04022471. https://doi.org/10.1061/(asce)mt.1943-5533.0004632.

[22] Morley PD, Royles R. Response of the Bond in Reinforced Concrete to High Temperatures. Mag Concr Res 1983;35:67–74. https://doi.org/10.1680/macr.1983.35.123.67.

[23] Bingöl AF, Tohumcu \.Ilhan. Effects of different curing regimes on the compressive strength properties of self compacting concrete incorporating fly ash and silica fume. Mater \& Des 2013;51:12–8.

[24] Cai B, Wu A, Fu F. Bond behavior of PP fiber-reinforced cinder concrete after fire exposure. Comput Concr An Int J 2020;26:115–25.

[25] Xiao J, Li Z, Xie Q, Shen L. Effect of strain rate on compressive behaviour of high-strength concrete after exposure to elevated temperatures. Fire Saf J 2016;83:25–37. https://doi.org/10.1016/j.firesaf.2016.04.006.

[26] Yu R, Spiesz P, Brouwers HJH. Development of an eco-friendly Ultra-High Performance Concrete (UHPC) with efficient cement and mineral admixtures uses. Cem Concr Compos 2015;55:383–94. https://doi.org/10.1016/j.cemconcomp.2014.09.024.

[27] Meng W, Khayat KH. Mechanical properties of ultra-high-performance concrete enhanced with graphite nanoplatelets and carbon nanofibers. Compos Part B Eng 2016;107:113–22. https://doi.org/10.1016/j.compositesb.2016.09.069.

[28] Ghaderi Barmi C, Saghafi MH, Golafshar A. Seismic retrofit of severely damaged beam-column RC joints using HPFRCC. Structures 2023;47:1020–32. https://doi.org/10.1016/j.istruc.2022.12.003.

[29] Peng GF, Yang WW, Zhao J, Liu YF, Bian SH, Zhao LH. Explosive spalling and residual mechanical properties of fiber-toughened high-performance concrete subjected to high temperatures. Cem Concr Res 2006;36:723–7. https://doi.org/10.1016/j.cemconres.2005.12.014.

[30] Khaliq W, Kodur V. Thermal and mechanical properties of fiber reinforced high performance self-consolidating concrete at elevated temperatures. Cem Concr Res 2011;41:1112–22. https://doi.org/10.1016/j.cemconres.2011.06.012.

[31] Way RT, Wille K. Effect of Heat-Induced Chemical Degradation on the Residual Mechanical Properties of Ultrahigh-Performance Fiber-Reinforced Concrete. J Mater Civ Eng 2016;28:04015164. https://doi.org/10.1061/(asce)mt.1943-5533.0001402.

[32] Yoo DY, Kim S, Kim JJ, Chun B. An experimental study on pullout and tensile behavior of ultra-high-performance concrete reinforced with various steel fibers. Constr Build Mater 2019;206:46–61. https://doi.org/10.1016/j.conbuildmat.2019.02.058.

[33] Krahl PA, de Miranda Saleme Gidrão G, Neto RB, Carrazedo R. Effect of curing age on pullout behavior of aligned and inclined steel fibers embedded in UHPFRC. Constr Build Mater 2021;266:121188.

https://doi.org/10.1016/j.conbuildmat.2020.121188.

[34] Liu F, Ding W, Qiao Y. Experimental investigation on the tensile behavior of hybrid steel-PVA fiber reinforced concrete containing fly ash and slag powder. Constr Build Mater 2020;241:118000. https://doi.org/10.1016/j.conbuildmat.2020.118000.

[35] Niu Y, Wei J, Jiao C. Crack propagation behavior of ultra-high-performance concrete (UHPC) reinforced with hybrid steel fibers under flexural loading. Constr Build Mater 2021;294:123510. https://doi.org/10.1016/j.conbuildmat.2021.123510.

[36] Moradikhou AB, Esparham A, Jamshidi Avanaki M. Physical & mechanical properties of fiber reinforced metakaolin-based geopolymer concrete. Constr Build Mater 2020;251:118965. https://doi.org/10.1016/j.conbuildmat.2020.118965.

[37] Tanyildizi H, Yonar Y. Mechanical properties of geopolymer concrete containing polyvinyl alcohol fiber exposed to high temperature. Constr Build Mater 2016;126:381–7. https://doi.org/10.1016/j.conbuildmat.2016.09.001.

[38] Qasim M, Lee CK, Zhang YX. An experimental study on interfacial bond strength between hybrid engineered cementitious composite and concrete. Constr Build Mater 2022;356:129299. https://doi.org/10.1016/j.conbuildmat.2022.129299.

[39] Varona FB, Baeza FJ, Bru D, Ivorra S. Evolution of the bond strength between reinforcing steel and fibre reinforced concrete after high temperature exposure. Constr Build Mater 2018;176:359–70. https://doi.org/10.1016/j.conbuildmat.2018.05.065.

[40] Basaran B, Kalkan I. Investigation on variables affecting bond strength between FRP reinforcing bar and concrete by modified hinged beam tests. Compos Struct 2020;242:112185. https://doi.org/10.1016/j.compstruct.2020.112185.

[41] Fakoor M, Nematzadeh M. Evaluation of post-fire pull-out behavior of steel rebars in high-strength concrete containing waste PET and steel fibers: Experimental and theoretical study. Constr Build Mater 2021;299:123917. https://doi.org/10.1016/j.conbuildmat.2021.123917.